Journal of Non-Newtonian Fluid Mechanics, 34 (1990) 129–144
Elsevier Science Publishers B.V., Amsterdam – Printed in The Netherlands

FLOW OF NON-NEWTONIAN FLUIDS IN A PIPE

F.T. PINHO and J.H. WHITELAW

Mechanical Engineering Department, Fluids Section, Imperial College of Science, Technology and Medicine, Exhibition Road, London SW7 2BX (U.K.)

(Received February 27, 1989; in revised form May 25, 1989)

Abstract

Measurements of mean axial velocity and of the three normal stresses have been obtained in fully developed pipe-flow with four concentrations of a polymer (sodium carboxymethyl cellulose) in aqueous solution and with water and viscous Newtonian fluids encompassing a range of Reynolds numbers from 240 to 111,000. The results quantify the delay in transition from laminar to turbulent flow caused by shear-thinning, the suppression of turbulent fluctuations particularly in the radial and tangential components of normal stress, and the drag reduction at the higher Reynolds numbers. They also confirm that the maximum drag reduction asymptote is appropriate to these shear-thinning solutions

1. Introduction

The emphasis of research into non-Newtonian flows has been to quantify the possible benefits of drag-reducing fluids and, for example, Berman [1] has reported measurements of the drag of dilute polymer solutions in pipe flows. Explanations of the related phenomena have been provided by, for example, Lumley [2] and Achia and Thompson [3], who discussed the effects of stretched molecules on the mechanisms of turbulence production. Earlier measurements with shear-thinning fluids include some local values of mean velocity and have been reviewed by Dodge and Metzner [4]. More recently, measurements of components of the Reynolds stress tensor have been reported in duct flows and Willmarth et al. [5], Patterson et al. [6] and Allan et al. [7] have confirmed that very dilute polymer solutions can cause damping of the radial and cross-flow normal stresses and increase in the

0377-0257/90/$03.50

axial normal stress very close to the wall. It is evident, however, that little has been done to examine systematically the velocity characteristics of shear-thinning fluids over a range of concentrations and encompassing laminar and turbulent flows, perhaps because of a combination of measurement difficulties and the immediate needs of drag reduction.

The present investigation stems from an interest in the mixing of non-Newtonian fluids in stirred tanks where, in practice, the fluids may be shear thinning with a wide range of viscosities including values in excess of 100 mPas. The previous investigations of Popiolek et al. [8] and Nouri [9] provide detailed information for Newtonian fluids agitated by an impeller as a function of rotational speed and impeller location and include consideration of dilute two-phase flows. Similar information is required for non-Newtonian fluids but should be preceded by an investigation which justifies the choice of fluid, documents the viscosity and provides a basis for understanding the relative importance of non-Newtonian and transitional effects. The latter are inevitable in stirred vessels where boundary layers form on the blades of the impeller and may influence the mixing processes. This information is likely to be particularly important to assist the process of scaling results of model investigations to the large vessels of industrial mixers and in the formulation of calculation methods to assist in this process.

The following section describes the pipe-flow configuration, laser velocimeter and fluids used to obtain measurements of mean velocity and normal stresses as a function of concentration of polymer and flow rate. The fluid, an aqueous solution of a straight-chain randomly coiled polymer, was selected after tests had been conducted with four alternative fluids (Pinho [10]) to quantify important properties, such as viscosity and its variation with shear rate and use in a flow rig. The third section presents results obtained for water, for a viscous Newtonian fluid, and for four concentrations of polymer in water, so as to encompass a range of viscosities from 3 to 180 mPas and bulk-flow velocities from 0.49 to 5.1 m/s corresponding to Reynolds numbers, based on the bulk velocity and the viscosity associated with the wall shear rate, from 240 to 111,000. The paper ends with a discussion of the relationship of the results to those of previous investigations and of their implications for mixer flows.

2. *Experimental arrangement*

The flow configuration is similar to that of Nouri et al. [11] and consisted of a vertical pipe of 25.4 mm inside diameter in a closed loop with one 60-litre tank and a centrifugal pump (Broadwall model 7). A 75 mm length section of honeycomb and a 20 mm internal diameter ring were located 90 diameters upstream of the transparent acrylic test section which had a

TABLE 1

Principal characteristics of the laser–Doppler velocimeter

Beam diameter of laser at e^{-2} intensity	0.65 mm
Focal length of lenses	
Imaging lens (nominal)	60 mm
Collimating lens (nominal)	300 mm
Focusing lens (nominal)	200 mm
Measured half angle of beams in air	8.90°
Calculated half angle of beams in	
water and CMC solutions	6.67°
viscous Newtonian fluid	6.41°
Fringe spacing	2.039 μm
Calculated dimensions of measuring volume in water at e^{-2} intensity	
minor axis	50 μm
major axis	424 μm
for viscous Newtonian fluid	
minor axis	50 μm
major axis	442 μm
Calculated number of stationary fringes	24
Frequency shift (MHz)	0.9 to 6.89
Short term stability of shift frequency (rms)	0.2%

polished internal surface and a square external cross-section to reduce optical diffraction. Static pressure holes of 0.5 mm inside diameter were arranged along the pipe at 410 mm and 15 mm intervals outside and inside the test section.

Velocity information was obtained with a laser-velocimeter which operated with a 5 mW helium–neon laser and light scattered by particles in the flow and collected at 20° from the forward direction. Frequency shift was provided by the rotation of a diffraction grating and the signals from the photomultiplier (EMI 9817 B) were processed by a counter (Heitor et al. [12]) interfaced to a microcomputer. The principal optical characteristics of the velocimeter and estimates of maximum uncertainties are listed in Tables 1 and 2, respectively.

Measurements of wall pressure and local values of mean axial velocity and the three normal stresses were obtained with water, a viscous Newtonian fluid and four aqueous solutions of the polymer. The polymer used was sodium carboxymethyl cellulose (CMC) grade 7H4C, manufactured by Hercules, at concentrations of 0.1, 0.2, 0.3 and 0.4% by weight and was chosen in preference to Carbopol, Aerosil and Viscarin for reasons of transparency, lower viscoelasticity, solution stability and facility of cleaning the rig and disposal of the fluid, as explained by Pinho [10]. To prevent bacteriological deterioration a biocide, Kathon CG manufactured by Rohm

TABLE 2

Estimates of uncertainties in measured quantities

Quantity	systematic	random
x, y positioning of measuring volume	$+100\ \mu$m	$\pm 200\ \mu$m
z positioning of measuring volume	–	$\pm 100\ \mu$m
x, y accuracy of milling table	–	$\pm 100\ \mu$m
z accuracy of milling table	–	$\pm 25\ \mu$m
U/U_0	$+3\%$ in steep gradient	$\pm 3\%$ in steep gradient
V/U_0, W/U_0	$1\%\ U/U_0$	$\pm 5\%$
$\langle u'^2 \rangle/U_0^2$, $\langle v'^2 \rangle/U_0^2$, $\langle w'^2 \rangle/U_0^2$	$+6\%$ in steep gradient	$\pm 3\%$
p	–	± 200 Pa

& Haas, was added at concentrations of 0.03 and 0.07 wt.% respectively to the two lower and the two higher concentration solutions.

The solutions were prepared in a 70 litre vessel, were mixed for more than four hours, and settled for more than eight hours prior to their use in the pipe rig to allow the complete hydration of the molecules. When added to the rig, the solutions were circulated for two or three periods of three minutes to remove trapped air and allowed to settle for a second eight hour period giving time for the air bubbles in suspension to come to the surface. Degradation of polymer solutions has been noted, for example, by Nakano and Minoura [14], who reported that the degradation occurred in inverse proportion to concentration and by Reddy and Singh [15], who showed that CMC has good stability with a 6% decrease in the viscosity of a 0.025 wt.% aqueous solution after two hours in a recirculating turbulent flow. The results of Pinho [10] show a 10% decrease in the viscosity of 0.4 wt.% CMC solutions after more than six hours at the highest flow rate of the present rig and more recent measurements led to similar results for 0.1 and 0.2 wt.% CMC solutions. It is also evident from the results of Pinho [10] that the elasticity of 0.4 wt.% CMC solutions could not be detected, as measured by normal stresses in a shear flow and by the stress-field distribution in small amplitude oscillatory shear flows.

The results of the following section were obtained with CMC solutions which were prepared as described above and used for not more than six hours, so that the viscosities of Fig. 1, and represented by the power law parameters of Table 3, can be expected to apply within, and usually well within, the 10% degradation. The temperature of the fluid within the pipe rig was maintained at $25 \pm 0.1°$C. It should also be noted that the refractive index of the 0.4 wt.% CMC solution was measured to be 1.333 at 25°C, identical to that of water. The thick Newtonian fluid was a 43% by weight aqueous solution of maltose syrup, Mor-Sweet grade 01511 manufactured by

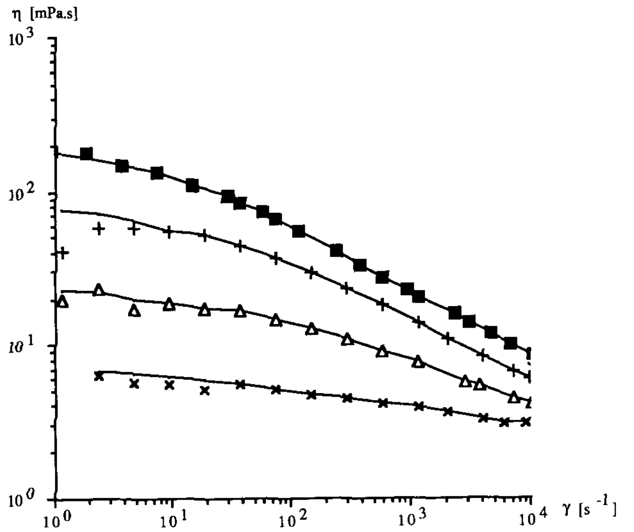

Fig. 1. Viscometric viscosity of CMC solutions at 25°C. × 0.1%, △ 0.2%, + 0.3%, and ■ 0.4% by weight.

Cerestar, with a density of 1134 kg/m^3, a kinematic viscosity of 4.77 mm^2/s and a refractive index of 1.389 at 25°C.

3. Results

The range of the flows investigated is shown by Table 4 which indicates the fluid, bulk-flow velocity, normalised centre-line velocity, Reynolds number (based on the bulk-flow velocity and the viscosity at the wall obtained from the measured pressure gradients and the solution of the integral momentum equation for pipe flow) and the drag reduction $dr = (\tau_s - \tau_w)/\tau_s$, where τ_s and τ_w are the wall shear stresses for the pure solvent and for the

TABLE 3

Power law, $\tau = K\gamma^n$, parameters and range of shear rate (γ)

Solution [a]	K (Pa·s)	n	γ range (s^{-1})
0.4% CMC	0.447	0.56	115–12,000
0.3% CMC	0.184	0.64	140–12,000
0.2% CMC	0.044	0.75	140–12,000
0.1% CMC	0.0075	0.90	140–12,000

[a] *By weight.*

TABLE 4

Pipe flow tests

Solution	U_b (m/s)	u_0/U_b	Re_{wa}	dr (%)
water	4.38	1.23	111,000	–
water	2.45	1.24	62,000	–
water	1.27	1.26	32,000	–
maltose	3.09	1.26	16,400	–
maltose	1.51	1.29	8,000	–
maltose	0.94	1.32	5,000	–
0.1%	5.12	1.19	43,000	59.8
0.1%	3.28	1.23	25,000	53.0
0.1%	2.28	1.24	17,000	46,8
0.1%	1.30	1.25	8,800	20.5
0.1%	0.82	1.33	5,100	2.4
0.1%	0.30	1.96	1.480	–
0.2%	5.10	1.25	30,000	65.6
0.2%	3.99	1.35	18,000	65.0
0.2%	3.11	1.39	12,000	64.0
0.2%	1.69	1.62	5,200	48.0
0.2%	0.85	1.85	2,060	–
0.2%	0.37	1.97	720	–
0.3%	4.93	1.36	15,000	66.4
0.3%	3.49	1.51	7,800	58.9
0.3%	1.21	1.82	1,550	–
0.4%	4.47	1.48	7,700	59.1
0.4% [a]	3.59	1.59	5,000	51.2
0.4% [a]	2.88	1.63	3,500	–
0.4% [a]	2.14	1.71	2,300	–
0.4% [a]	1.30	1.78	1,070	–
0.4% [a]	0.83	1.80	530	–
0.4% [a]	0.49	1.83	240	–

[a] From Pinho and Whitelaw [16].

solution flows at the same Reynolds number. This definition of Reynolds number was preferred to that of Metzner and Reed [13] which is based on laminar flow similarity rather than on the physical effects of viscosity on turbulent flow. All flows were fully developed in that the pressure gradients measured between wall holes immediately upstream of and around the test section were identical. The table shows that the effective viscosity increased with the concentration of CMC, so that, although bulk-flow velocities of around 5 m/s were achieved with all fluids, the maximum Reynolds number decreased from 111,000 with water to 7,700 with 0.4 wt.% CMC.

It is useful to note that Reynolds number effects are apparent with Newtonian fluids in duct flows at Reynolds numbers less than around

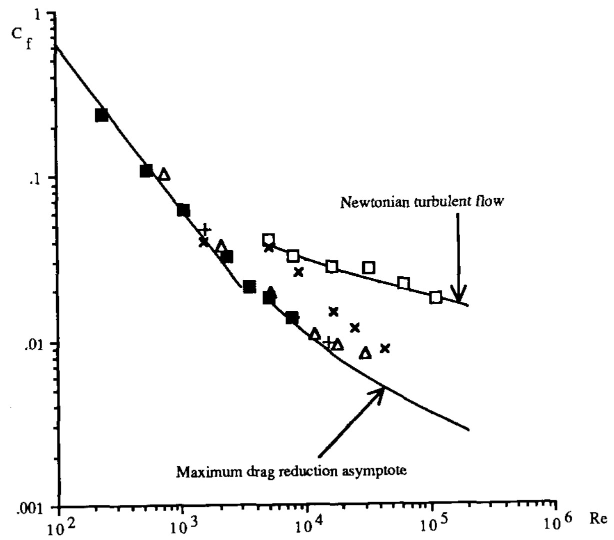

Fig. 2. Friction factor versus Reynolds number. × 0.1%, △ 0.2%, + 0.3%, ■ 0.4% CMC by weight, and □ Newtonian fluid (water and maltose syrup solution).

50,000, although they may be neglected for values higher than, say, 10,000. The results of Clark [17] and Hussain and Reynolds [18] together encompass a range from 10,000 to 130,000 and suggest that mean profiles plotted in wall coordinates have log-law regions independent of Reynolds number although fluctuating velocities in the near wall region are Reynolds number dependent. The earlier analysis of Patel and Head [19] considered Reynolds numbers from 1000 to 10,000 and showed (on the basis of mean-velocity profiles and wall-shear stress) the difficulty in defining flow regimes, since different criteria lead to different locations of the onset of fully developed turbulent flow which also differs for pipe and channel flows.

Figures 2 and 3 present values of skin-friction coefficient—$C_f = 2\ \Delta pD/(\rho u_b^2 L)$—and of normalised centre-line velocity—u_0/u_b—as functions of Reynolds number. The Newtonian results are consistent with previous work and confirm that the flow is close to being fully developed for Reynolds numbers above 5,000. The values of the skin-friction coefficient and of the normalised centre-line velocity suggest that 0.2, 0.3 and 0.4 wt.% CMC solution flows have an extended transition regime followed by turbulent results close to the maximum drag-reduction asymptote proposed by Virk et al. [20], while the 0.1 wt.% CMC solution after reaching turbulent flow at a Reynolds number of 5,000 appears to go through a similar form of drag reduction but with lower intensity. Conclusive evidence of the nature of the flow is not provided by Figs. 2 and 3 but turbulent flow might be associated with values of u_0/u_b less than 1.33, so that the flows of the 0.3 and 0.4 wt.%

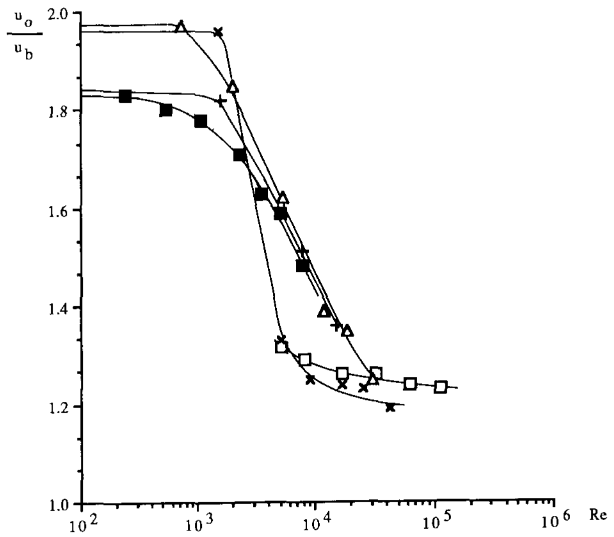

Fig. 3. Centreline velocity normalised with bulk velocity versus Reynolds number. × 0.1%, △ 0.2%, + 0.3%, ■ 0.4% by weight, and □ Newtonian fluid (water and maltose syrup solution).

CMC solutions can be regarded as transitional or laminar as can those with the 0.2 wt.% solution for Reynolds numbers below 10,000.

Local measurements of mean velocity and of the root-mean-square of velocity fluctuations are shown in Figs. 4 and 5 for 0.1 and 0.2 wt.% CMC solutions and on Figs. 6 and 7 to demonstrate the effects of CMC concentration at constant values of bulk velocity and Reynolds number.

The mean-velocity values of Figs. 4 and 5 are shown in physical and "law of the wall" coordinates. With the 0.1 wt.% CMC solution, the profile at the lowest Reynolds number of 1,480 is clearly not characteristic of turbulent flow, as would be expected, and the change in profile shape evident in physical coordinates is greater than would be expected for a Newtonian flow. The large deviation of the values of u^+ from the "law of the wall" for the three highest Reynolds numbers indicates a drag reduction related Reynolds number effect of the non-Newtonian fluid and Fig. 5 shows that this reduces as the increased concentration of the polymer causes the u^+ values to approach Virk's ultimate profile, and the results in physical coordinates show the delayed transition suggested by Figs. 2 and 3. The mean profiles of Fig. 5 and the skin-friction coefficients of Fig. 2 also agree in their confirmation that maximum drag reduction has been achieved with the 0.2 wt.% CMC solution.

The turbulence results of Figs. 4 and 5 immediately convey the information, consistent with the brief introductory review, that the maximum radial

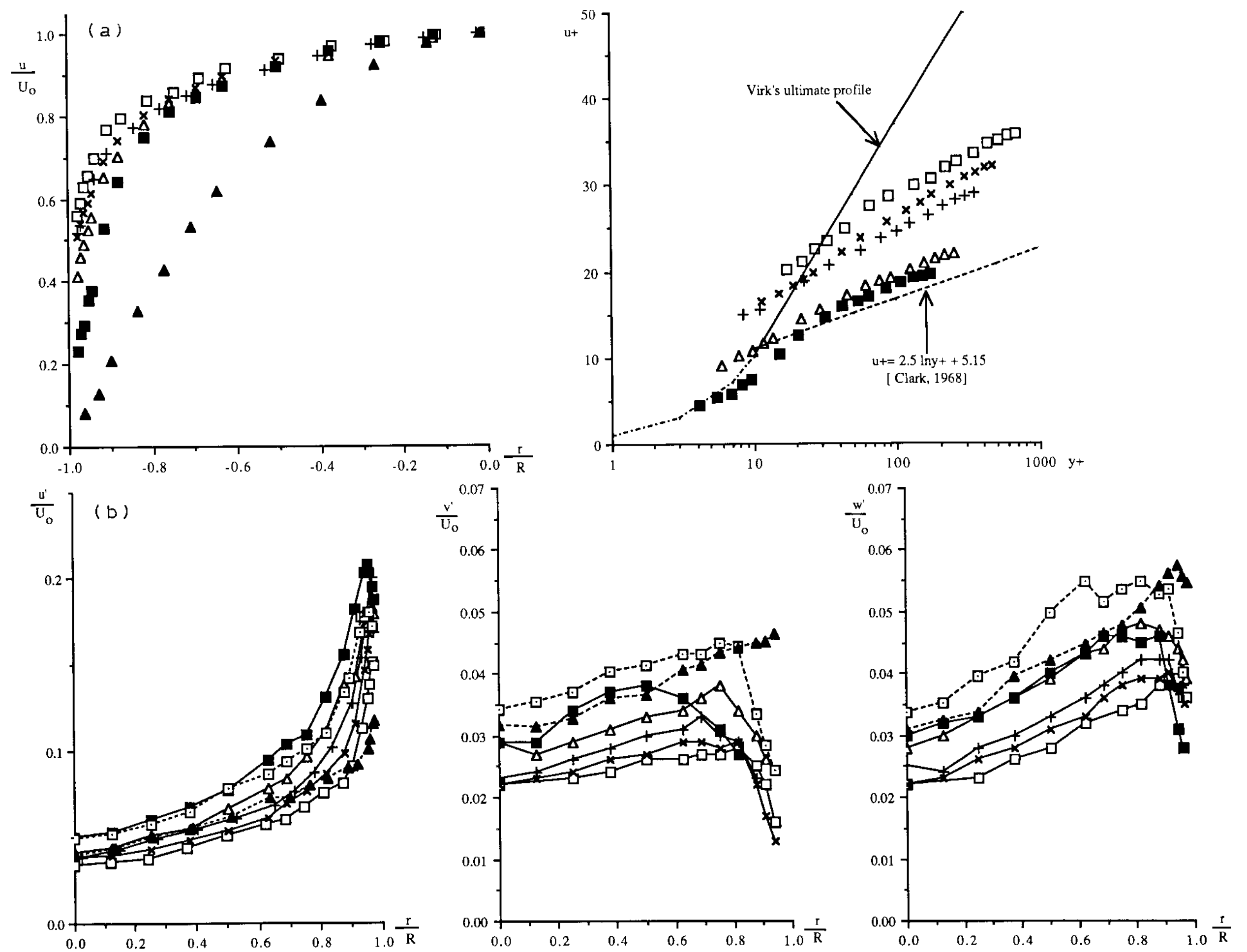

Fig. 4. (a) Mean velocity for 0.1 wt.% CMC. $Re_w = 1{,}480$ ▲; 5,070 ■; 8,800 △; 16,800 +; 25,200 ×; and 43,000 □. (b) Root-mean-square of axial, radial and tangential velocity fluctuations for 0.1 wt.% CMC. $Re_w = 5{,}070$ ■——■; 7,800 △——△; 16,800 +——+; 25,200 ×——×; 43,000 □——□; Newtonian fluid 5,000 ⊡- - - - -⊡; 111,000 ▲- - - - - -▲.

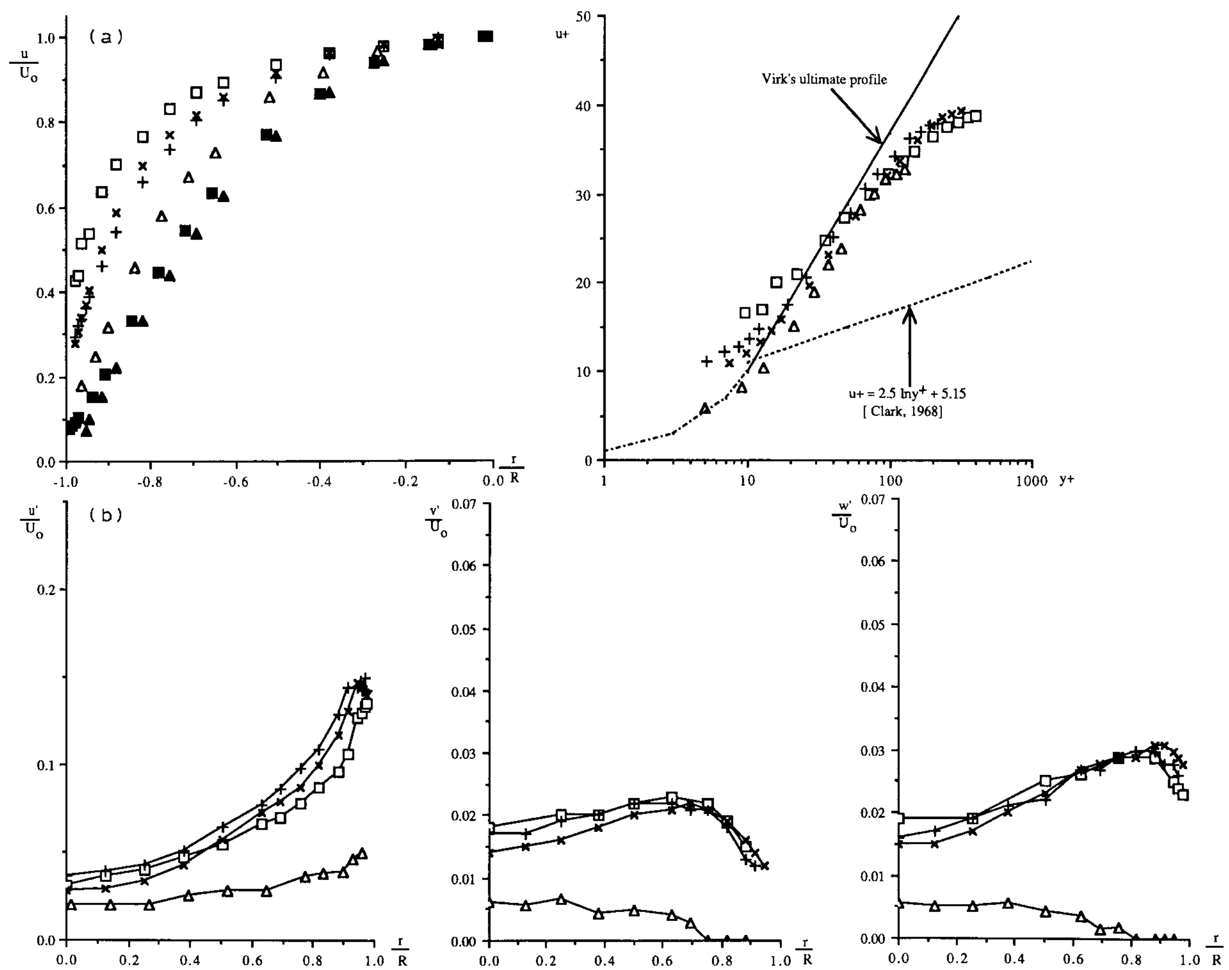

Fig. 5 (a) Mean velocity profiles for 0.2 wt.% CMC. $Re_w = 720$ ▲, 2,600 ■; 5,200 △; 12,000 +; 18,000 ×; and 30,000 □. (b) Root-mean-square of axial, radial and tangential velocity fluctuations for 0.2 wt.% CMC. For caption see Fig. 5(a).

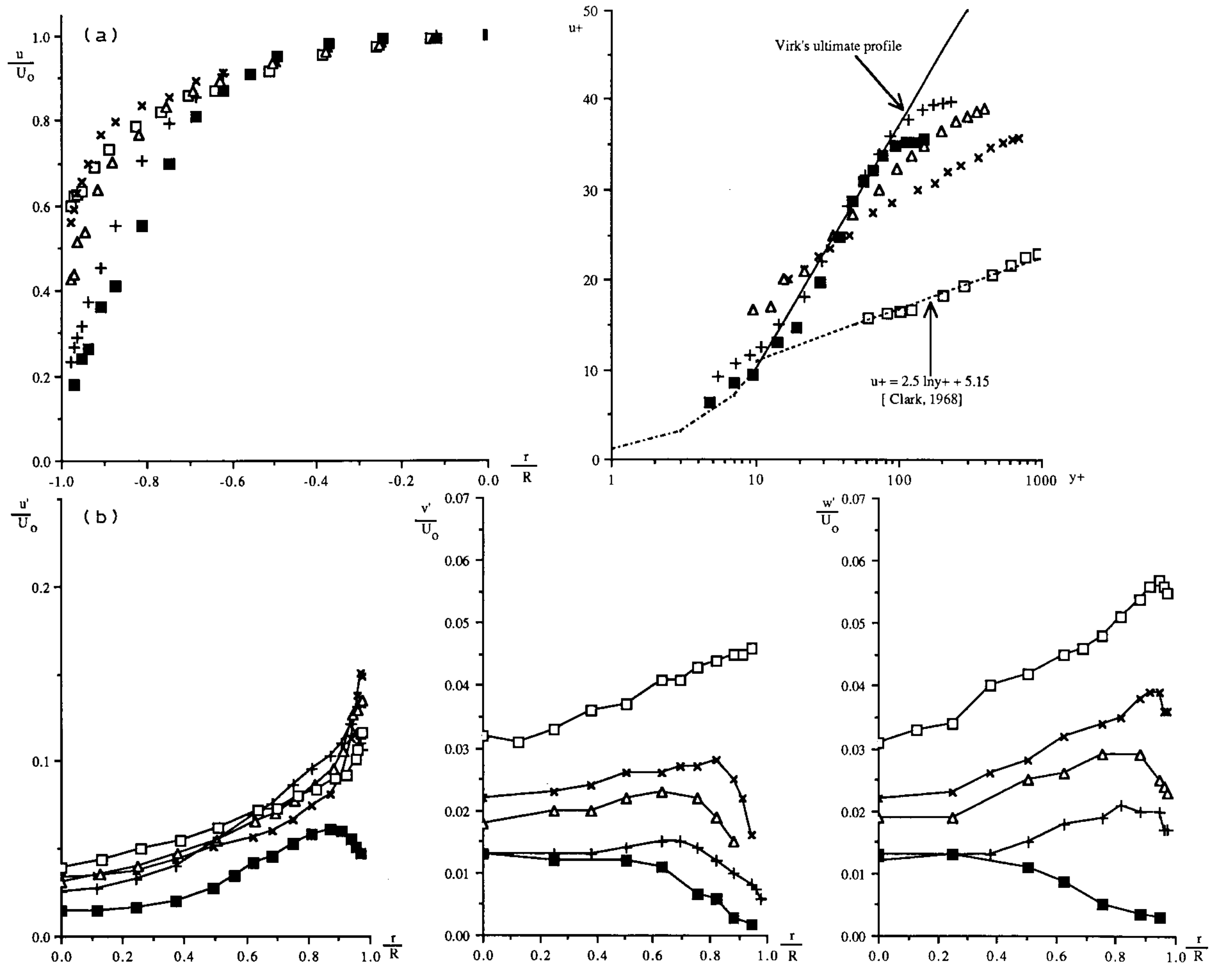

Fig. 6 (a) Mean velocity profiles for a bulk velocity of 4.8 m/s. □ Newtonian; × 0.1%; △ 0.2%; + 0.3%; ■ 0.4% CMC by weight. (b) Root-mean-square of axial, radial and tangential velocity fluctuations. For caption see Fig. 6(a).

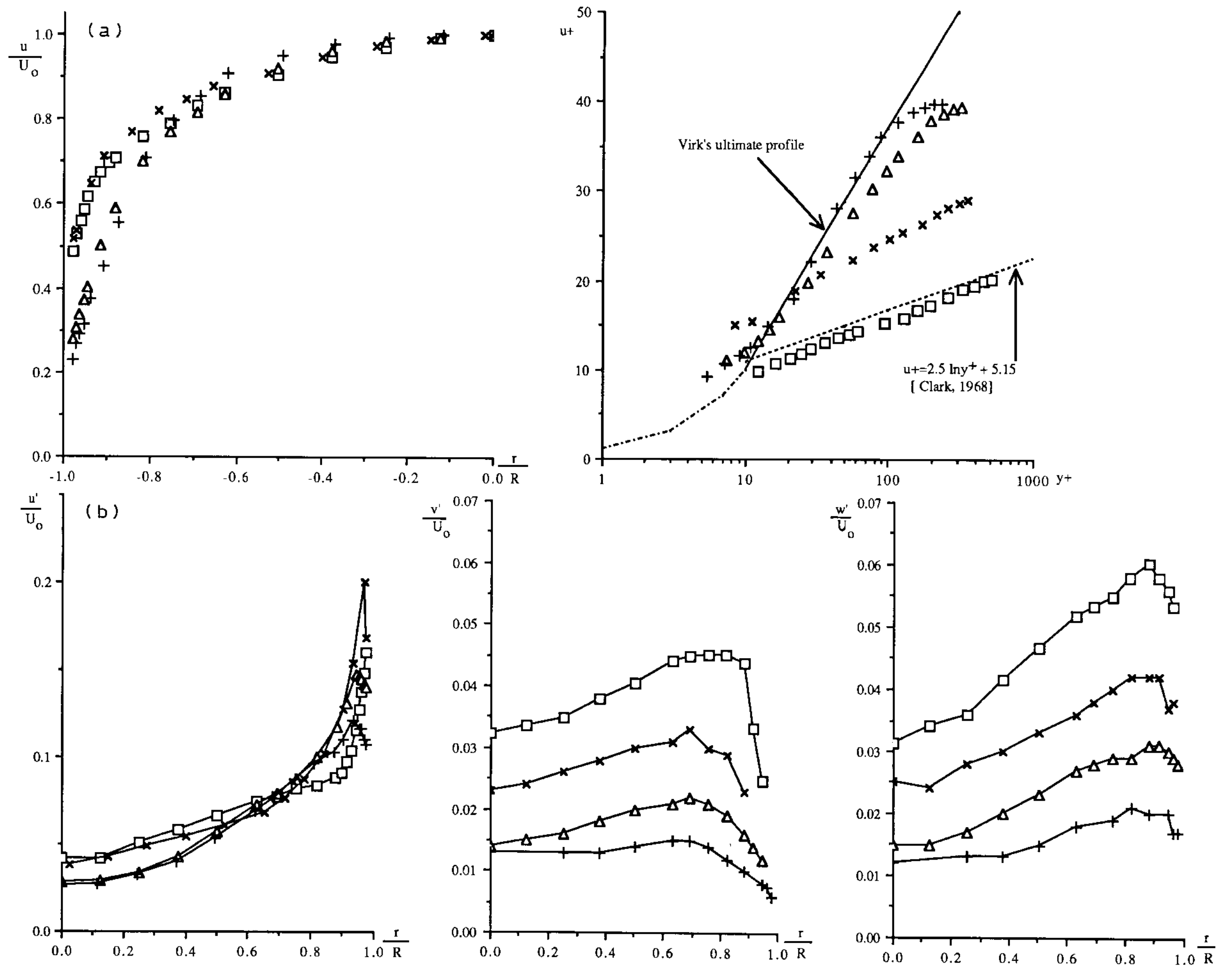

Fig. 7 (a) Mean velocity profiles at $Re_w = 16{,}700$. □ Newtonian fluid, × 0.1%, △ 0.2%, and + 0.3% by weight. (b) Root-mean-square of axial, radial and tangential velocity fluctuations at $Re_w = 16{,}700$. For caption see fig. 7(a).

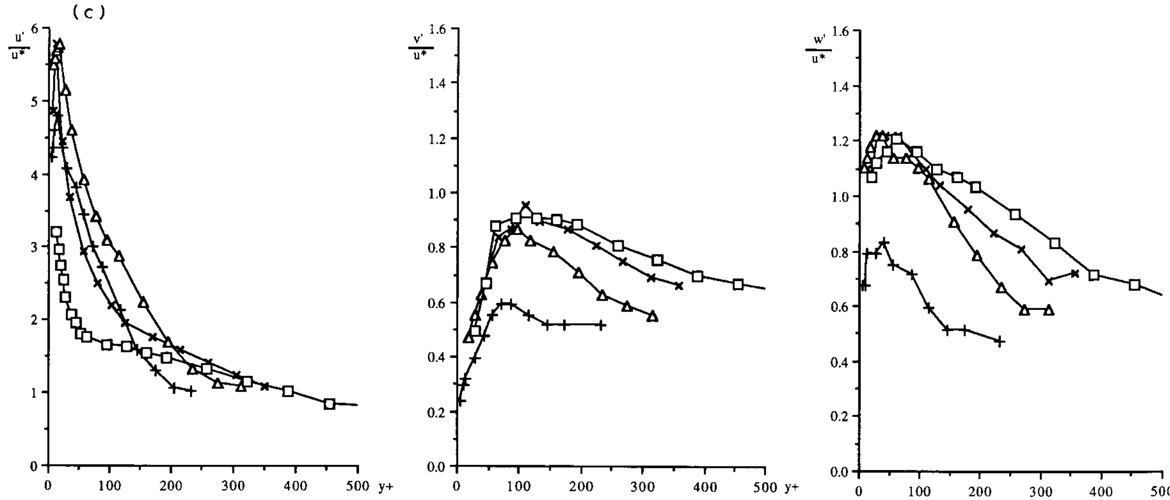

Fig. 7(c). Root-mean-square of axial, radial and tangential velocity fluctuations at $Re_w = 16{,}700$. For caption see fig. 7(a).

and tangential velocity fluctuations are around five times less than those of the axial velocity fluctuations and considerably less than those associated with a Newtonian fluid, plotted for comparison in Fig. 4(b) at Reynolds numbers of 5,000 and 111,000. The delayed transition associated with the 0.2 wt.% CMC solution is even more apparent in the intensity values, clearly evident at a Reynolds number of 5,200. Both sets of results suggest that the maximum fluctuation intensities are achieved at low Reynolds numbers in the transition or turbulent regimes particularly in the absence of drag reduction, and for the lowest polymer concentrations.

The previous figures have considered the effect of concentration of the polymer as a function of Reynolds number even though it is known that this non-dimensional representation of the ratio of inertial to viscous forces is not fully representative of non-Newtonian fluids where the viscosity varies with strain rate, as in Fig. 1. Thus, Fig. 6 shows the effect of concentration of the polymer for a fixed flow rate of 4.8 m/s, and a constant 60–65% drag reduction for the polymer solutions. The suppression of turbulence is clear in the mean-flow profiles, except that the 0.1 wt.% CMC solution results in a slightly fuller physical profile than that with water, already apparent in Fig. 3, and in spite of a Reynolds number which is around half. None of the solutions give results close to the "law of the wall" and all approach Virk's ultimate profile, which is a maximum for the 0.3 wt.% solution. The 0.4 wt.% CMC solution again shows the extended transition in terms of low levels of turbulence and the flatness of the mean velocity profile.

The results of Fig. 7 correspond to a Reynolds number of around 16,700 and, in terms of mean and root-mean-square of the fluctuations of the axial velocity, show a smaller spread than those of Fig. 6, even when allowance is made for the absence of results with the 0.4 wt.% CMC solution and differences in drag reduction intensity. There is also less spread in the radial and tangential intensity levels, especially evident when normalised by the friction velocity and for values of the dimensionless wall distance y^+ below 150 (Fig. 7c). At higher values of y^+, the decrease in the ratio of inertia to viscous forces associated with shear thinning might explain the growing scatter of u'/u^* for the different cases. This possibility also appears to be supported by similar results plotted for a Reynolds number of 8,100.

4. Discussion

Aqueous solutions of CMC are sufficiently transparent to allow measurements with laser velocimetry and have viscosities from 3 to 180 mPas over a range of strain ratios from 1 to 10^4 s^{-1} and constant within 10% when circulated by a pump for periods of six hours. Transition from laminar to turbulent flow is extended so that, for example, a 0.2 wt.% CMC solution does not achieve turbulent flow below a Reynolds number of around 10,000 and a 0.4 wt.% CMC solution has turbulence intensities less than half those of a Newtonian fluid at a Reynolds number of 7,700. Perhaps of greatest importance is that the present rig allowed a Reynolds number of 110,000 with water flow in contrast to a maximum value of 7,700 with a 0.4 wt.% CMC, so that turbulent flow could not be achieved with this non-Newtonian fluid.

It can be anticipated, therefore, that stirred reactors will not derive the same benefits from turbulent-flow mixing when the fluid has non-Newtonian properties similar to that of 0.4 wt.% CMC, and correspondingly improved mixing as the concentration of the polymer is reduced. This is likely to manifest itself in the boundary layer on the blades of the impeller so that, for example with a Rushton-type arrangement, the boundary-layers will tend to remain laminar with early separation and impaired performance. Where the boundary-layer remains attached, small-scale turbulence in particular will be suppressed even where the flow achieves a length Reynolds number sufficient to ensure turbulence and, more likely, will be greatly suppressed or absent. Of course, much of the mixing of stirred reactors may not depend on the details of the flows on the blades of the impeller, and macro-mixing will be achieved by pressure, inertial and viscous forces. This is supported by experiments currently under way which show that the flow of water and of 0.2 wt.% CMC over a confined baffle leads to separated-flow regions of similar size and with similar maximum negative normalised velocities, even though the corresponding Reynolds numbers are three times different.

The arguments about stretched molecules and their preferential effect on Reynolds normal stresses other than those associated with the main flow direction are further supported by the present measurements which also suggest that the maximum drag reduction asymptote is approached with a 0.2 wt.% CMC solution. It is also confirmed that both Virk's maximum drag reduction asymptote and ultimate profile are appropriate to these shear-thinning solutions. There seems little advantage in solutions of polymer concentrations greater than 0.2 wt.% if the reason for their use is associated with shear-thinning.

Acknowledgement

We are glad to acknowledge financial support from a Brite project involving the European Commission, ICI plc. and Unilever Research, and helpful cooperation with colleagues in these organisations and at Imperial College. F.P. would particularly like to thank Dr. J.M. Nouri for his constant support and understanding.

References

1 N.S. Berman, Drag reduction by polymers, Ann. Rev. Fluid Mech., 10 (1978) 47.
2 J. Lumley, Drag reduction in two phase and polymer flows, Phys. Fluids., 20 (1977) S64.
3 B.U. Achia and D.W. Thompson, Structure of the turbulent boundary layer in drag reducing pipe flow, J. Fluid Mech., 81 (1977) 439.
4 D.W. Dodge and A.B. Metzner, Turbulent flow of non-Newtonian systems, AICHE J., 5 (1959) 189.
5 W.W. Willmarth, T. Wei and O. Lee, Laser anemometer measurements of Reynolds stress in a turbulent channel flow with drag reducing polymer additives, Phys. Fluids, 30 (1987) 933.
6 G.K. Patterson, J. Chosnek and J.L. Zakin, Turbulence structure in drag reducing polymer solutions, Phys. Fluids, 20 (1977) S89.
7 J.J. Allan, C.A. Greated and W.D. McComb, Laser anemometer measurements of turbulent structure in non-Newtonian fluids, J. Phys (D): Appl. Phys., 17 (1984) 533.
8 Z. Popiolek, M. Yianneskis and J.H. Whitelaw, An experimental study of the steady and unsteady flow characteristics of stirred reactors, J. Fluid Mech., 175 (1987) 537.
9 J.M. Nouri, Single and two-phase flows in ducts and stirred reactors, PhD Thesis, University of London, London, 1988.
10 F. Pinho, Characteristics of non-Newtonian fluids, Imp. Coll., Mech. Eng. Dept. report FS/87/35, London, 1987.
11 J.M. Nouri, J.H. Whitelaw and M. Yianneskis, Particle motion and turbulence in dense two-phase flows, Int. J. Multiphase Flow, 13 (1987) 729.
12 M.V. Heitor, J. Laker and C. Vafidis, Instruction manual for the FS model 2 Doppler frequency counter, Imp. Coll., Mech. Eng. Dept. Report FS/84/10, London, 1984.
13 A.B. Metzner and J.C. Reed, Flow of Non-Newtonian fluids—Correlation of the laminar, transition and turbulent flow regions, AICHE J., 1 (1955) 434.
14 A. Nakano and Y. Minoura, Effects of solvent and concentration on scission of polymers with high speed stirring, J. Appl. Polym. Sci., 19 (1975) 2119.
15 G.V. Reddy and R.P. Singh, Drag reduction effectiveness and shear stability of polymer–polymer and polymer–fibre mixtures in recirculatory turbulent flow of water, Rheol. Acta, 24 (1985) 296.
16 F. Pinho and J.H. Whitelaw, Flow characteristics of a non-Newtonian fluid, Proc. 4th. Int. Symp. on Appl. of Laser Anem. to Fluid Mech., Paper 20.1, Lisbon, 1988.
17 J.A. Clark, A study of incompressible turbulent boundary-layers in channel flow, J. Bas. Eng., 90 (1968) 455.
18 A.K.M.F. Hussain and W.C. Reynolds, Measurements in fully developed turbulent channel flows, J. Fluids Eng., 97 (1975) 568.
19 V.C. Patel and M.R. Head, Some observations on skin-frictions and velocity profiles in fully developed pipe and channel flows, J. Fluid Mech., 38 (1969) 181.
20 P.S. Virk, H.S. Mickley and K.A. Smith, The ultimate asymptote and mean flow structure in Tom's phenomena, J. Appl. Mech., 37 (1970) 488.